



14 **Abstract**

15 Additive manufacturing (3D printing) permits the fabrication of tablets in shapes unattainable  
16 by powder compaction and so the effects of geometry on drug release behavior is easily  
17 assessed. Here, tablets (printlets) comprising of paracetamol dispersed in polyethylene  
18 glycol were printed using stereolithographic 3D printing. A number of geometric shapes were  
19 produced (cube, disc, pyramid, sphere and torus) with either constant surface area (SA) or  
20 constant surface area/volume ratio (SA/V). Dissolution testing showed that printlets with  
21 constant SA/V ratio released drug at the same rate, while those with constant SA released  
22 drug at different rates. A series of tori with increasing SA/V ratio (from 0.5 to 2.4) were  
23 printed and it was found that dissolution rate increased as the SA/V ratio increased. The  
24 data show that printlets can be fabricated in multiple shapes and that dissolution  
25 performance can be maintained if the SA/V ratio is constant or that dissolution performance  
26 of printlets can be fine-tuned by varying SA/V ratio. The results suggest that 3D printing is  
27 therefore a suitable manufacturing method for personalized dosage forms.

28

29 **Key words:**

30 3D printing; additive manufacturing; Paracetamol; tablets; stereolithographic

31

32 **Introduction**

33 The development of new actives with high potencies and narrow therapeutic indices  
34 combined with the increasing desire for personalisation of medicines (in terms of dose  
35 strength and/or drug combinations) are driving factors changing the landscape of  
36 pharmaceutical manufacturing, compelling the pharmaceutical industry to consider new  
37 methods of pharmaceutical production. The advent of 3D printing (3DP), and the range of  
38 technologies developed, has resulted in a new era of additive manufacturing approaches in  
39 which material is deposited layer-by-layer to fabricate solid objects. 3DP offers many  
40 qualities ideally suited to meet the challenges facing the pharmaceutical sector; small  
41 production runs, infinite variability of dose and/or drug combinations and the possibility to  
42 use a wide range of excipients to solubilise, target or control drug release (1).

43

44 The kinetics of drug release from oral dosage forms can be influenced by different  
45 parameters including dimension and shape (2-4). Karasulu et al (5) found that the dissolution  
46 rate from erodible polymeric tablets containing theophylline was affected by the geometrical  
47 shape, polymer ratio and inclusion of diluents in the formulation, concluding that geometry  
48 played an important role in determining drug release rates. Raju et al (6) also reported that  
49 the drug release from hydrophilic polymeric tablets was directly related to the surface area to  
50 volume ratio (SA/V) of the tablets.

51

52 One limitation of these studies is that to create multiple tablet geometries requires production  
53 of specific molds. In this aspect, 3D printing offers great potential, because it allows the  
54 fabrication of varied and complex shapes, designed with computer-aided design (CAD)  
55 software (1, 7-9). Previously (10), we investigated the effect that geometry had on the drug  
56 release of paracetamol-loaded (4% wt./wt.) polyvinylalcohol (PVA) 3D printed tablets  
57 (Printlets<sup>®</sup>). Using a fused deposition modeling (FDM) 3D printer we fabricated printlets in 5  
58 geometric shapes that would have been difficult to achieve with traditional powder  
59 compaction. The results showed surface area to volume ratio (SA/V) was the dominant

60 factor influencing drug release. However, variations in drug release rates between  
61 geometries were seen because erosion of the tablet occurred during dissolution.

62

63 In this work, we explore the effect of geometry on drug release from cross-linked polymeric  
64 printlets, created with stereolithography (SLA) 3D printing. With this technology a laser is  
65 focused into a resin tank, causing photopolymerization of the resin. By moving the laser in a  
66 raster pattern, objects can be created in a layer-by-layer fashion. To enhance the speed of  
67 photopolymerization a photoinitiator (PI) is used. A PI absorbs energy to produce an  
68 initiating species (often a free radical) which is then able to first attack a monomer and then  
69 add consecutively other monomers to this growing polymer chain (11). Since this process  
70 occurs in three dimensions, it yields a crosslinked network. Additional excipients (not  
71 involved in the photopolymerization process) can become entrapped in the crosslinked  
72 network, enabling the possibility of fabricating drug-loaded tablets.

73

#### 74 **Materials and methods**

75 Polyethylene glycol diacrylate (PEGda, average MW 700), diphenyl(2,4,6-trimethylbenzoyl)  
76 phosphine oxide (TPO) and paracetamol were purchased from Sigma Aldrich Ltd (UK). The  
77 salts for preparing the buffer dissolution media were purchased from VWR International Ltd.,  
78 Poole, UK. All materials were used as received.

79

80 *Resin preparation:* PEGda was used as the photopolymerizable resin, TPO was used as the  
81 photoinitiator (2% wt./wt.) and paracetamol was used as a model drug (4% wt./wt.). Briefly,  
82 TPO was added to PEGda and kept protected from light with constant stirring until complete  
83 dissolution (approximately 45 min). Paracetamol was added next and stirring continued until  
84 complete dissolution (approximately 25 minutes), the mixture was then transferred into the  
85 resin tray of the printer to begin the fabrication of the tablets.

86

87 *3D printing:* All printlets were fabricated with a Formlabs 1+ SLA 3D printer (Formlabs Inc,  
88 USA). The printer is equipped with a 405nm laser and can fabricate objects with a resolution  
89 of 300 microns and a layer thickness of 25, 50, 100 or 200 microns. The electronic shapes  
90 (Figure 1) were designed with AutoCAD® 2017 and exported as a stereolithography file (.stl)  
91 into the 3D printer software (PreForm Software v. 2.11.1 Formlabs Inc.). The parameters of  
92 the printer were set to flexible resin (version 01) with a layer thickness of 0.05 mm. The  
93 dimensions of the printlets were measured using an electronic calliper (0.150 mm PRO-  
94 MAX, Fowler, mod S 235 PAT).

95

96 *Scanning electron microscopy (SEM):* Surface and cross-section images of the printlets  
97 were taken with an SEM (JSM-840A Scanning Microscope, JEOL GmbH, Eching, Germany).  
98 All samples for SEM testing were coated with carbon (~30–40 nm).

99

100 *Drug loading:* To determine drug concentrations of the printlets, they were crushed using a  
101 mortar and pestle and then dissolved in 1 L of deionized water with constant magnetic  
102 stirring for 24 h. Samples of the solutions were then filtered through 0.45 µm filters (Millipore  
103 Ltd., Ireland). The amount of drug in solution was determined using HPLC (Hewlett Packard  
104 1050 Series HPLC system, Agilent Technologies, UK). The assay entailed a mobile phase  
105 consisting of water (85%) and methanol (15%), through an Eclipse Plus C18 5µm column,  
106 15 x 4.6 cm (Agilent, USA). The mobile phase was pumped at a flow rate of 1 ml/min and the  
107 eluent was screened at a wavelength of 247 nm. The injection volume was 20 µL and the  
108 temperature was kept at ambient. The measurements were made in triplicate.

109 *Dynamic dissolution testing conditions:* Drug dissolution profiles for the 3D printed tablets  
110 were obtained with a USP-II apparatus (Model PTWS, Pharmatest, Germany). The  
111 hydrogels were placed in 750 mL of 0.1 M HCl for 2 h to simulate the gastric compartment,  
112 and then transferred into 950 mL of modified Hanks (mHanks) bicarbonate physiological  
113 medium for 35 min (pH 5.6 to 7); 3) and then in modified Krebs buffer (1000ml) (pH 7 to 7.4  
114 and then to 6.5). The modified Hanks buffer based dissolution medium (12) forms an in-situ

115 modified Kreb's buffer (13) by addition of 50 mL of pre-Krebs solution to each dissolution  
116 vessel. These conditions mimic transit through the small intestinal and colonic environments.  
117 The buffer capacity and ionic composition of the physiological bicarbonate buffers also  
118 closely match the buffer capacities of the intestinal fluids collected from different parts of the  
119 gut in humans (12-15). The paddle speed of the USP-II was fixed at 50 rpm, and the tests  
120 were conducted at 37 +/-0.5 °C (n=3). The percentage of drug released from the  
121 formulations was determined using HPLC, using the same method as described above.

122

123 Statistical analysis was performed using IBM SPSS Statistics 22 software. Comparison of  
124 means of drug release during 10 h was analysed using one-way ANOVA repeated  
125 measures, followed by Tukey HSD Post Hoc Test. P < 0.05 was considered as a significant  
126 level. To evaluate the relationship between drug release with weight and SA/V, simple and  
127 multiple regression analysis were performed.

128

129 *SA/V change*: the change in SA/V ratio was calculated by measuring the initial dimensions of  
130 the printlets and after placing them in 0.1 M HCl for 2 h, then in modified Hanks (mHanks)  
131 bicarbonate physiological medium during 22 h at 37 °C to simulate the dissolution test  
132 conditions. The final SA/V ratio was calculated using equation 1.

133

134 
$$Final \frac{SA}{V} (\%) = \frac{SA/V_s}{SA/V_i} \times 100 \quad \text{Eq 1}$$

135 Where:

136  $SA/V_s$  = SA/V for the swollen tablets (after 24 h).

137  $SA/V_i$  = Initial SA/V.

138 *Swelling ratio (SR)*: Printlets were blotted with filter paper to remove any uncured liquid  
139 formulation on the surface immediately following printing, then they were weighed ( $W_i$ ). After  
140 this, printlets were placed into HCl (0.1 M) for 2h then into modified Hanks (mHanks)

141 bicarbonate physiological medium for 8 h; after this, the excess water was carefully wiped off  
142 and the tablets were weighed ( $W_s$ ). The SR was calculated using equation 2.

143

$$144 \quad SR = \frac{W_s}{W_i} \quad \text{Eq 2}$$

145 Where:

146  $W_s$  = weight of the swollen tablet (after 24 h).

147  $W_i$  = initial weight of the tablet.

148

## 149 **Results.**

150

151 Paracetamol was readily dissolved in PEGDa, yielding a clear solution similar to the results  
152 obtained by Wang et al and Martinez et al (16-17), and the laser was able to photocure the  
153 resin. Figures 2-4 show the various printlets produced and it is apparent that the SLA printer  
154 was able to fabricate them with good resolution. Tables 1 and 2 quantify the physical  
155 dimensions of the printlets, all of which were close to the target values set in the CAD  
156 designs. SEM images of the printlets (Figure 5) do not show any visible pores, indicating that  
157 the resin photocured with a high crosslinking density.

158

159 The average drug content in the printlets was  $3.82 \pm 0.12$  % w/w (the expected content  
160 based on the resin formulation was 4% w/w) and no degradation peaks were seen in the  
161 HPLC chromatograms. This result suggests that there is little drug degradation during  
162 printing, which was to be expected since SLA printing involves no significant rise in  
163 temperature and paracetamol does not degrade under light. This is a potential benefit of SLA  
164 printing compared with fused deposition modelling (FDM) printing; the latter involves  
165 appreciable rises in temperature and has been shown to cause significant drug degradation  
166 when used to fabricate polymeric tablets (18). The slightly lower than expected concentration

167 might be due to incomplete drug extraction from the crosslinked printlet prior to HPLC  
168 analysis; this is an issue seen previously by Wang et al (16).

169

170 Figures 6 and 7 show the drug release profiles from the printlets with similar SA and SA/V  
171 ratios. Printlets with similar initial surface areas did not show similar drug release profiles;  
172 statistical analysis of the data showed that drug release was significantly different for the  
173 sphere (which had the lowest value for SA/V) compared with almost all of the other shapes,  
174 except the cylinder. Drug release from the cylinder was significantly different only from the  
175 pyramid (which has the highest SA/V ratio). In the case of printlets with similar initial SA/V  
176 ratios, the results showed that the percentage of drug released from any shape were not  
177 significantly different ( $p= 0.05$ ).

178

179 In our previous work (10) it was also noted that the mass of the tablets could influence the  
180 drug release kinetics. In this work we performed simple and multiple regression to compare  
181 the relation and possible influence that both the SA/V and weight may have on the drug  
182 release kinetics. The multiple regression equation is:

183

$$184 \quad \text{Drug release } 10h = -1.573 + 60.9.SA/V - .014weight$$

185

186 This means that drug release increases on average by 60.9 units as the SA/V value  
187 increases by one, after adjusting for weight. The coefficient for weight is -.055 in the simple  
188 regression and -.014 in the multiple regression, hence adjusting for SA/V decreases the  
189 effect of weight on drug release. Weight is significant in the simple regression ( $p\text{-value}=$   
190  $.002$ ) but not in the multiple regression ( $p\text{-value}= .350$ ). The coefficient for SA/V is 67.9 in  
191 the simple regression and 60.9 in the multiple regression, hence adjusting for weight  
192 decreases the effect of SA/V on drug release. SA/V is significant in both, the simple and the  
193 multiple regression ( $p\text{-value}= 0.000$  on both). Therefore, SA/V is an important characteristic  
194 to predict the speed of drug release after adjusting for weight. The adjusted R square is



195 0.604, suggesting that approximately 60% of the variation in drug release is explained by its  
196 linear relationship with weight and SA/V.

197

198 The physical parameters of the printlets are shown in Tables 1 and 2. The results show that  
199 as the SA/V increases, the speed of drug release does as well. This is in agreement with  
200 other studies; Parojčić et al (19) reported that the drug release kinetics from carbomer matrix  
201 tablets can be controlled by modifying the type and content of polymer and the geometry of  
202 tablets. In particular, they concluded that the relative surface area (absolute surface  
203 area/absolute volume) is a reliable parameter to compare the drug release kinetics from  
204 tablets of different shapes. Tablet surface area/volume has also been found to be the most  
205 relevant parameter determining the rate of drug release from hydroxypropylmethylcellulose  
206 (HPMC) matrix tablets and lipid tablets (2, 20).

207

208 Since SA/V ratio has an important influence on the speed of drug release from 3DP tablets,  
209 a group printlets with a range of different initial SA/V ratios were printed, in order to compare  
210 their speed of drug release. All the printlets for this section of the study were tori, as this is  
211 the geometry that can be altered to give the widest range of SA/V ratios. Additionally, as  
212 noted by Wang et al (16), a torus is a complex shape that would be difficult to fabricate using  
213 conventional techniques and it is a shape that has been studied for the possibility to produce  
214 tablets with a zero-order release (21-22). To achieve a SA/V ratio greater than 1.4 it was  
215 necessary to print a tablet comprised of multiple tori; Table 3 shows the physical parameters  
216 of the printlets. Again, the flexibility of 3D printing facilitates the simple manufacture of these  
217 very complex shapes.

218

219 Figure 8 shows the results of drug dissolution for the printlets with different SA/V ratios. The  
220 data show that drug release becomes faster as the SA/V increases, confirming the  
221 observation reported above that among the parameters affecting drug release kinetics, SA/V  
222 plays an important role. It is also clear from these data that 3D printing is a new approach to

223 pharmaceutical manufacturing that allows precise tailoring of dissolution profiles through  
224 changing geometry rather than by altering the composition of the formulation.

225

## 226 **Conclusion**

227

228 SLA 3DP is suitable for fabricating complex drug-loaded tablets with a good resolution. The  
229 results from this work show that of all the geometric parameters, SA/V ratio has the greatest  
230 influence on the drug release kinetics from PEGda printlets. One immediate benefit of this  
231 outcome is that it will be possible to adjust the dose of printlets so that they are tailored to  
232 the needs of an individual patient, but that by changing SA/V ratio the specific drug release  
233 profile can be maintained.

234

## 235 **References**

236

237 (1) Trenfield SJ, Awad A, Goyanes A, Gaisford S, Basit AW. 3D Printing Pharmaceuticals:  
238 Drug Development to Frontline Care. *Trends Pharmacol Sci* 2018.  
239 doi:10.1016/J.TIPS.2018.02.006.

240 (2) Gökçe EH, Özyazici M, Ertan G. The effect of geometric shape on the release properties  
241 of metronidazole from lipid matrix tablets. *J Biomed Nanotechnol.* 2009;5:421–427.  
242 doi:10.1166/jbn.2009.1052

243 (3) Karasulu HY, Ertan G. Different geometric shaped hydrogel theophylline tablets:  
244 statistical approach for estimating drug release. *Farmaco.* 2002;57:939–945.

245 (4) Skoug JW, Borin MT, Fleishaker JC, Cooper AM. In Vitro and in Vivo Evaluation of  
246 Whole and Half Tablets of Sustained-Release Adinazolam Mesylate. *Pharm Res.*  
247 1991;8:1482–1488. doi:10.1023/A:1015834114359

- 248 (5) Karasulu HY, Ertan G, Köse T. Modeling of theophylline release from different  
249 geometrical erodible tablets. *Eur J Pharm Biopharm.* 2000;49:177–182.
- 250 (6) Raju PN, Prakash K, Rao TR, Reddy BCS, Sreenivasulu V, Narasu ML. Effect of Tablet  
251 Surface Area and Surface Area / Volume on Drug Release from Lamivudine Extended  
252 Release Matrix Tablets. *Int J Pharm Sci Nanotechnol.* 2010;3:872–876.
- 253 (7) Ventola CL. Medical Applications for 3D Printing: Current and Projected Uses. *Pharmacy  
254 Therapeutics.* 2014;39:704–11.
- 255 (8) Fina F, Goyanes A, Gaisford S, Basit AW. Selective laser sintering (SLS) 3D printing of  
256 medicines. *Int J Pharm.* 2017;529:285-293. doi: 10.1016/J.IJPHARM.2017.06.082
- 257 (9) Goyanes A, Scarpa M, Kamlow M, Gaisford S, Basit AW, Orlu M. Patient acceptability of  
258 3D printed medicines. *Int J Pharm.* 2017;530:71–8. doi:10.1016/j.ijpharm.2017.07.064.
- 259 (10) Goyanes A, Martinez PR, Buanz A, Basit A, Gaisford S. Effect of geometry on drug  
260 release from 3D printed tablets. *Int J Pharm.* 2015;494:657-663.  
261 doi:10.1016/j.ijpharm.2015.04.069
- 262 (11) Fouassier JP, Lalevée J. Photopolymerization and Photo-Cross-Linking, in:  
263 Photoinitiators for Polymer Synthesis. Wiley-VCH Verlag GmbH & Co. KGaA, Weinheim,  
264 Germany, 2012 p. 3–9. doi:10.1002/9783527648245.ch1
- 265 (12) Liu F, Merchant HA, Kulkarni RP, Alkademi M, Basit AW. Evolution of a physiological  
266 pH 6.8 bicarbonate buffer system: application to the dissolution testing of enteric coated  
267 products. *Eur J Pharm Biopharm.* 2011;78:151–157. doi:10.1016/j.ejpb.2011.01.001
- 268 (13) Fadda HM, Merchant HA, Arafat BT, Basit AW. Physiological bicarbonate buffers:  
269 stabilisation and use as dissolution media for modified release systems. *Int J Pharm.*  
270 2009;382:56-60. doi:10.1016/j.ijpharm.2009.08.003

271 (14) Goyanes A, Hatton GB, Basit AW. A dynamic in vitro model to evaluate the intestinal  
272 release behaviour of modified-release corticosteroid products. *J Drug Deliv Sci Technol.*  
273 2014;25:36–42. doi:10.1016/j.jddst.2014.12.002

274 (15) Goyanes A, Hatton GB, Merchant HA, Basit AW. Gastrointestinal release behaviour of  
275 modified-release drug products: dynamic dissolution testing of mesalazine formulations. *Int J*  
276 *Pharm.* 2015;484:103–108. doi:10.1016/j.ijpharm.2015.02.051

277 (16) Wang J, Goyanes A, Gaisford S, Basit AW. Stereolithographic (SLA) 3D printing of oral  
278 modified-release dosage forms. *Int J Pharm.* 2016;503:207–212.  
279 doi:10.1016/j.ijpharm.2016.03.016

280 (17) Martinez PR, Goyanes A, Basit AW, Gaisford S. Fabrication of Drug-Loaded Hydrogels  
281 with Stereolithographic 3D Printing. *Int J Pharm.* 2017;532:313–7.  
282 doi:10.1016/j.ijpharm.2017.09.003.

283 (18) Goyanes A, Buanz ABM, Hatton GB, Gaisford S, Basit AW. 3D printing of modified-  
284 release aminosalicylate (4-ASA and 5-ASA) tablets. *Eur J Pharm Biopharm.* 2014;89:157–  
285 62. doi:10.1016/j.ejpb.2014.12.003

286 (19) Parojčić J, Durić Z, Jovanović M, Ibrić S. An investigation into the factors influencing  
287 drug release from hydrophilic matrix tablets based on novel carbomer polymers. *Drug Deliv.*  
288 2004;11:59–65. doi:10.1080/10717540490265379

289 (20) Reynolds TD, Mitchell S, Balwinski KM. Investigation of the effect of tablet surface  
290 area/volume on drug release from hydroxypropylmethylcellulose controlled-release matrix  
291 tablets. *Drug Dev Ind Pharm.* 2002;28:457–66. doi:10.1081/DDC-120003007

292 (21) Kim C. Compressed Donut-Shaped Tablets with Zero-Order Release Kinetics. *Pharm*  
293 *Res.* 1995;12:1045–1048. doi:10.1023/A:1016218716951

294 (22) Kim C. Release kinetics of coated, donut-shaped tablets for water soluble drugs. *Eur J*  
295 *Pharm Sci.* 1999;7:237–242.

296

Shape	Surface area (mm <sup>2</sup> )	Volume (mm <sup>3</sup> )	SA/V ratio	Weight (mg)	Density (mg/mm <sup>3</sup> )
Cylinder	284.0 ± 6.8	321.1 ± 13.3	0.885 ± 0.016	403.0 ± 3.8	1.26 ± 0.05
Sphere	260.2 ± 6.0	394.7 ± 13.7	0.659 ± 0.008	559.0 ± 13.4	1.42 ± 0.02
Pyramid	253.4 ± 0.9	220.3 ± 1.6	1.150 ± 0.004	346.1 ± 4.5	1.57 ± 0.01
Torus	278.4 ± 3.6	276.1 ± 7.4	1.009 ± 0.015	358.7 ± 2.3	1.30 ± 0.04
Cube	292.6 ± 2.1	340.6 ± 3.7	0.859 ± 0.003	404.7 ± 6.9	1.19 ± 0.02

297

298 **Table 1. Various physical parameters for printlets with similar surface areas**

299

300

<b>Shape</b>	<b>Surface area (mm<sup>2</sup>)</b>	<b>Volume (mm<sup>3</sup>)</b>	<b>SA/V ratio</b>	<b>Weight (mg)</b>	<b>Density (mg/mm<sup>3</sup>)</b>
Cylinder	210.8 ± 3.4	222.8 ± 7.0	0.946 ± 0.017	274.7 ± 1.4	1.23 ± 0.05
Sphere	116.9 ± 1.9	118.9 ± 2.9	0.984 ± 0.008	142.0 ± 4.0	1.19 ± 0.01
Pyramid	283.5 ± 11.1	281.3 ± 16.6	1.009 ± 0.019	424.7 ± 35.4	1.51 ± 0.04
Torus	278.4 ± 3.6	276.1 ± 7.4	1.009 ± 0.015	358.7 ± 2.3	1.30 ± 0.04
Cube	213.6 ± 4.6	212.5 ± 6.8	1.006 ± 0.011	268.4 ± 6.2	1.26 ± 0.02

301






302 **Table 2. Various physical parameters for printlets with similar initial SA/V ratios**

303

304

305

---

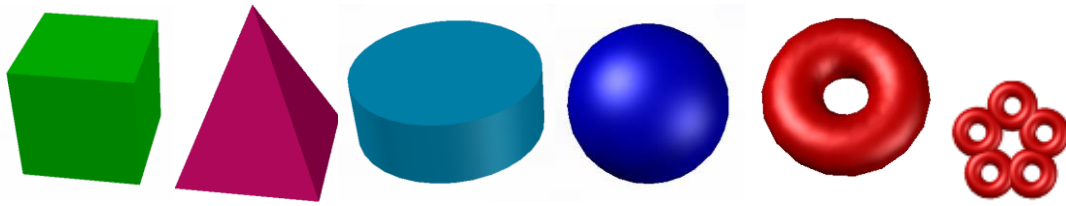
Physical Parameter					
SA (mm <sup>2</sup> )	1263.3	575.8	276.4	278.6	190.5
V (mm <sup>3</sup> )	2526.6	823.4	276.4	197.8	78.0
SA/V	0.5	0.7	1	1.4	2.4
Weight (mg)	3388.0	1029.8	358.7	490.3	102.3
	(RSD 4.1%)	(RSD 3.6%)	(RSD 0.6%)	(RSD 2.0%)	(RSD 1.5%)

---

306

307 **Table 3. Various physical parameters of the group of tori with different SA/V ratios**

308



309

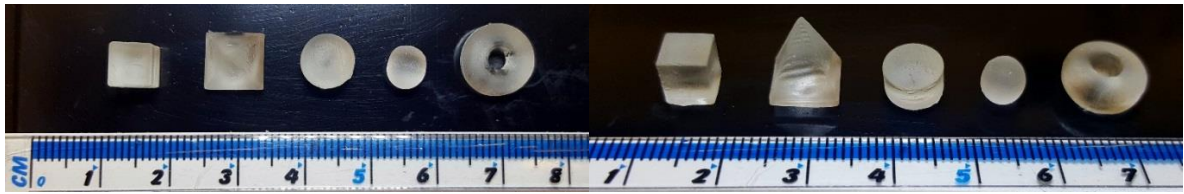
310 **Figure 1. CAD drawings of the printlets used to explore the effect of geometry on drug**

311 **release**

312

313



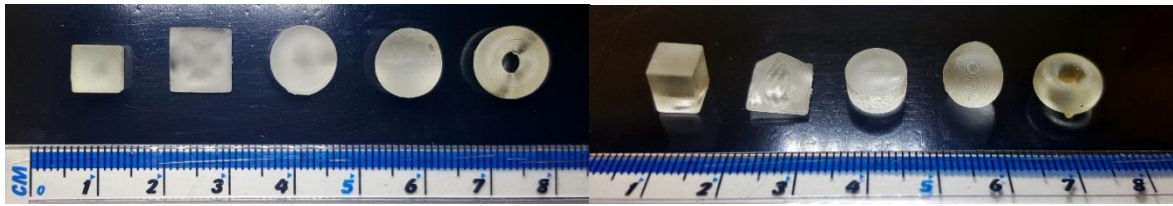


314

315 **Figure 2. Printlets with similar initial SAV ratios**

316

317

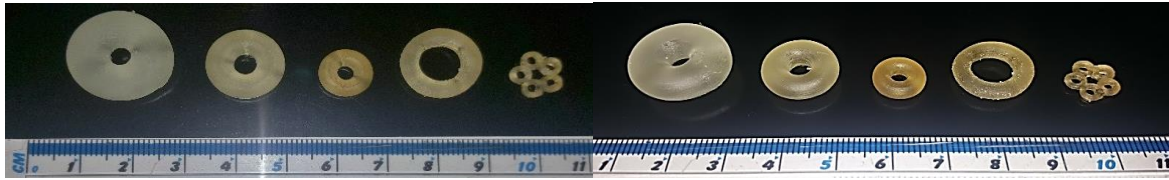


318

319 **Figure 3. Printlets with similar initial surface areas**

320

321

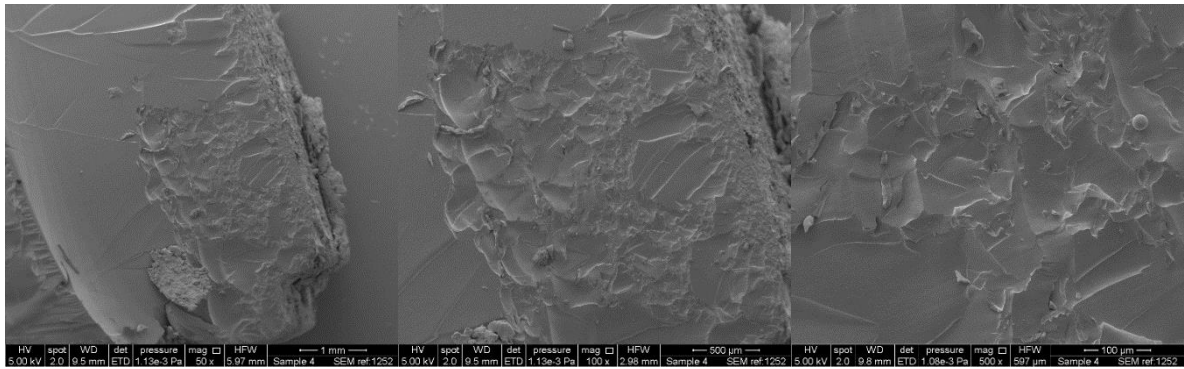


322

323 **Figure 4. Torus printlets with different SAV ratios**

324

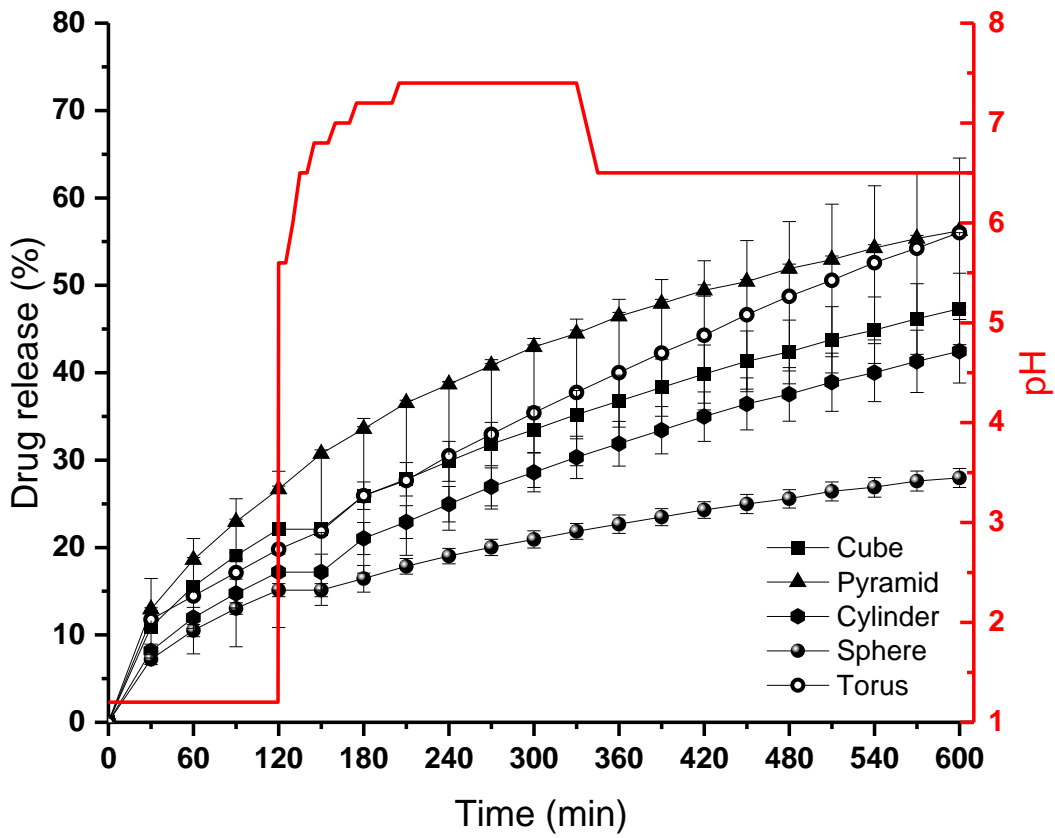
325



326

327 **Figure 5. SEM images of the printlets, showing surface detail**

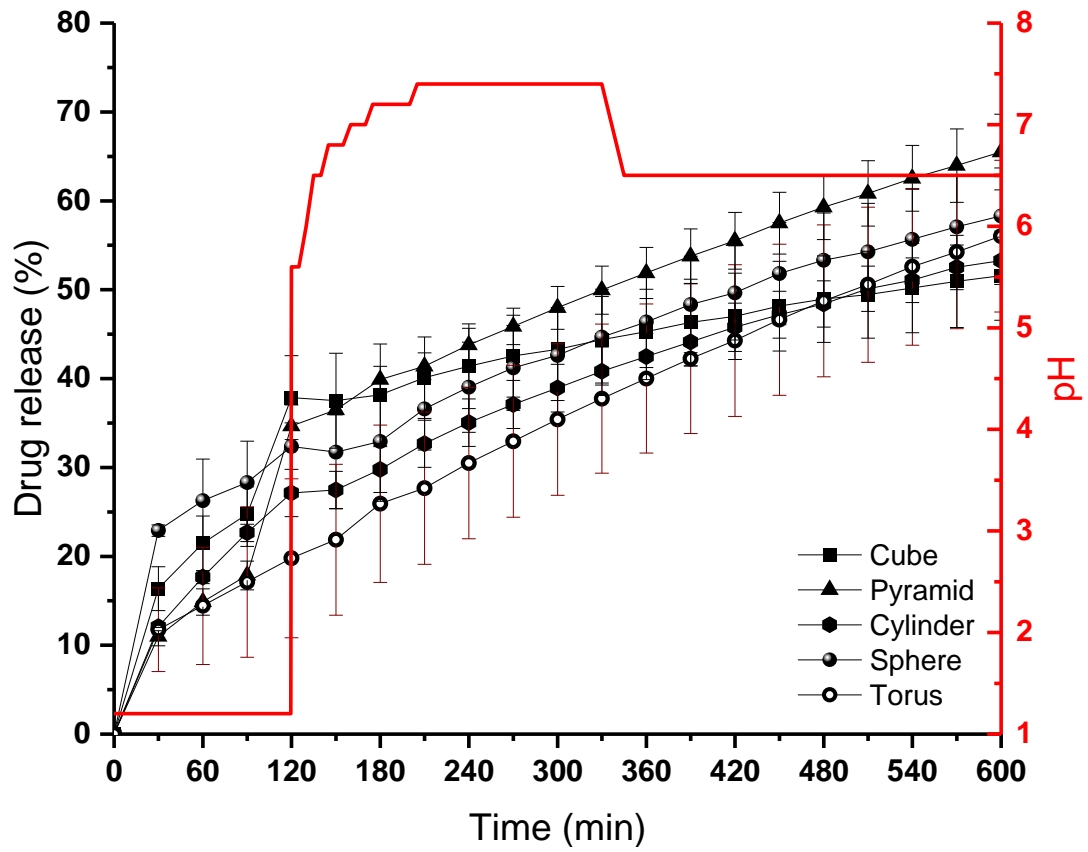
328



329

330 **Figure 6. Dissolution profiles for printlets with similar surface areas**

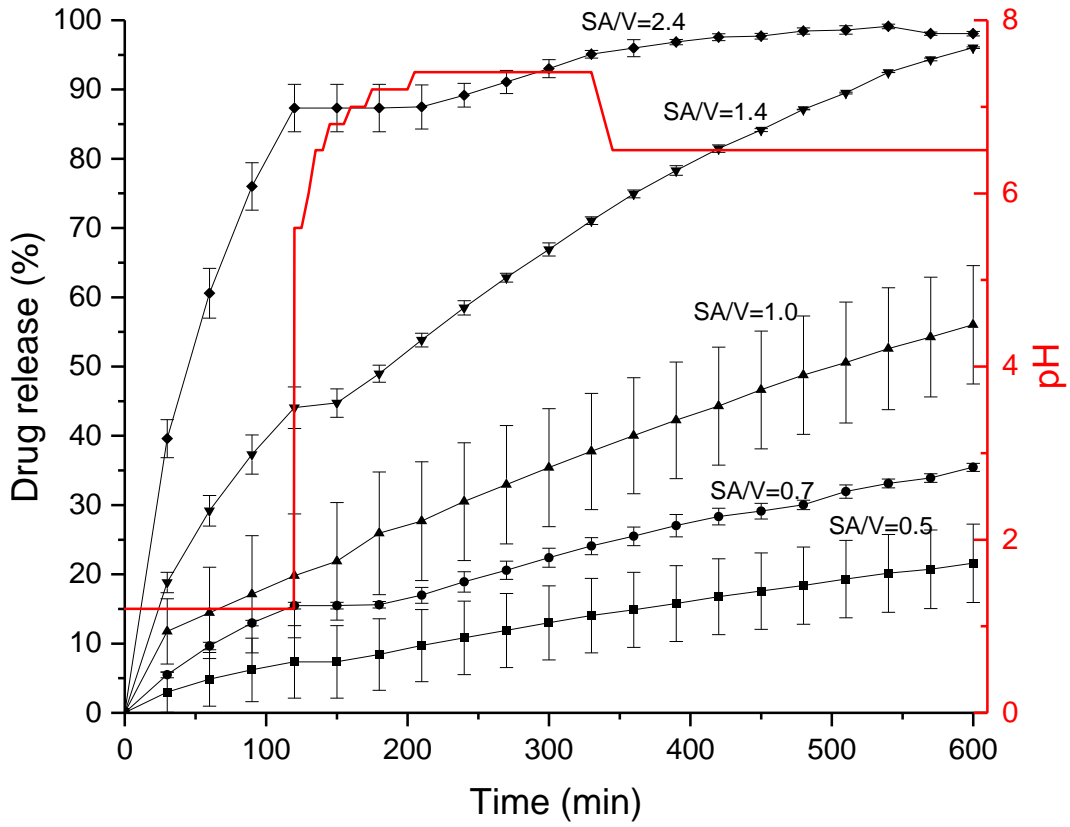
331



332

333 **Figure 7. Dissolution profiles for printlets with similar SA/V ratios**

334



335

336 **Figure 8. Drug release from torus printlets with different SA/V ratios**